NASA Technical Memorandum 105576

Derated Ion Thruster Design Issues

Michael J. Patterson and
Vincent K. Rawlin
Lewis Research Center
Cleveland, Ohio

Prepared for the
22nd International Electric Propulsion Conference
co-sponsored by the AIDAA, AIAA, DGLR, and JSASS
Viareggio, Italy, October 14–17, 1991

NASA

DERATED ION THRUSTER DESIGN ISSUES

Michael J. Patterson* and Vincent K. Rawlin†
National Aeronautics and Space Administration
Lewis Research Center

Preliminary activities to develop and refine a lightweight 30 cm engineering-model ion thruster are discussed. The approach is to develop a "derated" ion thruster which is a thruster capable of performing both auxiliary and primary propulsion roles over an input power range of at least 0.5-5.0 kW. Design modifications to a baseline thruster to reduce mass and volume are discussed. Performance data over an order-of-magnitude input power range are presented, with emphasis on the performance impact of engine throttling. Thruster design modifications to optimize performance over specific power envelopes are discussed. Additionally, lifetime estimates based on weartest measurements are made for the operating envelope of the engine.

Introduction

An activity has been initiated at the NASA Lewis Research Center (LeRC) to develop a ~7.0 kg engineering-model xenon ion thruster. The objective of this thruster development effort is to produce a 30 cm engine design capable of performing both auxiliary and primary propulsion functions over a input power range of at least 0.5-5.0 kW, while requiring minimal or no design modifications necessary to perform either role. For auxiliary propulsion, this derated approach virtually eliminates known life-limiting issues, increases the thrust-to-power ratio, and reduces flight qualification times while demonstrating a thruster approach capable of performing higher power auxiliary and primary propulsion functions.[1]

A potential disadvantage of this derated approach for auxiliary propulsion is thruster integration on mass and volume constrained spacecraft. This is because the 30 cm thruster is larger and more massive than conventional ion thruster approaches to auxiliary propulsion.[1]

The impact of thruster mass and size on the ion propulsion system can be illustrated by the following simple analyses. The use of derated 30 cm ion thrusters to provide 15 years of stationkeeping capability for a 1600 kg-class three-axis stabilized communications satellite has been shown to yield significant performance and lifetime advantages over propulsion systems using smaller ion thrusters.[1,2] However, some disadvantages are incurred including: a larger and more massive (~70 kg) propulsion system which reduces the net mass benefit of using ion propulsion by about 140 kg compared to that of reference 3; and a larger (about double) envelope of energetic beam ions, especially in the near-field where concerns of ion impingement on solar array and other spacecraft surfaces are greatest.

The mass model of reference 2 was used to show the sensitivity of spacecraft mass at geosynchronous transfer orbit (GTO) to variations in ion thruster mass, for spacecraft equipped with stationkeeping ion propulsion. Figures 1 and 2 show the calculated propulsion system dry mass (without contingency) and the spacecraft mass in GTO, respectively, as a function of the mass of the ion thruster. Also shown in Fig. 1 are values of propulsion system dry mass obtained from the literature for a number of different ion thrusters proposed for a variety of stationkeeping missions.[3-11]

These data show that in general the propulsion system dry mass decreases rapidly as the thruster mass decreases.

*Aerospace Engineer, member AIAA

†Aerospace Engineer, member AIAA

The results of the mass model (Fig. 2) indicate that the spacecraft mass delivered to GTO decreases more than 17 kg-per-kilogram reduction in thruster mass. This strong sensivity occurs because there are four thrusters per propulsion system, each with a gimbal having an assumed mass of 34 percent of the thruster mass. In addition, decreased thruster and gimbal masses require less structure, contingency, and propellant for stationkeeping, attitude control, and orbit transfer. The reduced spacecraft mass in GTO yields a one-for-one increase in the net mass benefit of using ion propulsion for stationkeeping. Consequently it is of benefit to reduce ion thruster mass.

This paper presents preliminary results obtained from a mass optimization activity conducted with the laboratory model 30 cm ion thruster. Additionally, performance and lifetime assessments are made for the power throttling range of the derated ion thruster.

Design Modifications

The mass-breakdown of the baseline 30 cm laboratory model derated ion thruster, excluding the external plasma screen and cabling, is shown in Fig. 3. As indicated the most massive subassembly of the thruster is the discharge chamber, followed by the ion optics. The total thruster mass is approximately 10.7 kg, which compares favorably to that of the engineering model J-series divergent-field thruster mass of 10.4 kg[12], and the XIPS 25 cm thruster mass of 12.1 kg.[5] This section discusses design modifications to the derated thruster discharge chamber to reduce mass and volume, and modifications to other subassemblies to optimize engine performance.

Discharge Chamber

The discharge chamber includes the steel discharge shell, the permanent magnets used to create the ring-cusp field, and integration hardware to mount the ion optics and gimbal assembly. The steel discharge chamber for the baseline thruster, and other conventional ring-cusp thrusters, performs several functions including acting as the principle structural element of the thruster, acting as a plasma containment vessel for the discharge plasma, and providing a return flux path for the magnetic circuit. In providing a return flux path for the permanent magnets, the ferromagnetic chamber walls influence the magnetic flux density internal and external to the thruster discharge.

The shape of the volume magnetic field inside the discharge chamber can have a first-order impact on discharge, and overall thruster, stability and performance. The magnetic field in a ring-cusp thruster performs at least 3 functions including increasing the primary electron containment length, controlling the effective anode surface area for electron current collection, and (at the cusp) filtering low energy electrons to the anode while containing the primary electrons in the discharge. While analytical tools are under development to predict the discharge performance sensitivity to changes in magnetic field[13,14], discharge performance in the past has been correlated on a qualitative basis to the shape of the volume magnetic field as characterized by scalar magnetic field contour plots.

A series of tests were conducted to characterize the impact of chamber wall material and magnet size on discharge volume magnetic field and discharge chamber performance. Figures 4 and 5 show scalar magnetic field contour plots for the baseline thruster with 1.5 mm and 0.75 mm thick steel chamber wall thicknesses respectively. Both plots have the same line contour frequency, and indicate only a minor change in volume field. As indicated in the discharge chamber performance curves of Fig. 6, no significant impact in discharge chamber performance (or stability) was observed over the indicated range in beam current, corresponding to an input power range of approximately 1.1 kW to 5.5 kW.

An additional experiment was conducted to reduce discharge chamber mass by reducing the size (width) of the permanent magnets used in the discharge by 50% from the baseline size. The scalar magnetic field plot for this configuration with the 0.75 mm steel chamber wall thickness is shown in Figure 7. Figure 7 indicates a considerable reduction in the scalar flux density in the bulk volume of the chamber, which might imply higher loss rate of electron current at the magnet cusps and reduced discharge chamber performance. As indicated in Fig. 8, a plot of discharge chamber performance for the two magnet sizes, a modest increase in baseline discharge losses was experienced with the smaller magnets. However at the high propellant efficiencies of interest for thruster operation, this impact is negligible. Additional data were obtained with the reduced magnet size and 1.5 mm thick steel chamber wall confirming this trend.

A final test was conducted to map the scalar magnetic field of a discharge chamber constructed of non-ferromagnetic material, using the standard magnet layout as used on the baseline thruster. Although performance data for this thruster geometry is not yet available, an examination of the contour plots for both full-size and reduced-size magnets indicate bulk volume fields comparable to those of the 0.75 mm thick steel chamber, indicating the potential of obtaining high discharge chamber performance without the requirement for ferromagnetic materials of a minimum thickness. Consequently, the use of thin, low-density, high thermal conductivity, and possibly non-ferromagnetic, discharge chamber material is anticipated. This, in combi-

nation with the use of reduced-size permanent magnets will effect a reduction in discharge chamber and overall thruster mass by approximately 80% and 40% respectively.

A potential disadvantage of reducing wall thickness and/or eliminating the steel chamber material is an increase in the magnetic flux external to the engine. These stray magnetic fields may impact the thruster performance, and the host spacecraft. In the case of the thruster performance, stray magnetic fields in the region of the neutralizer have been demonstrated to impede the neutralizer-beam coupling process.[15,16] To address this issue, magnetic field maps were made external to the thruster at the location of peak density, and are plotted in Fig. 9 for the non-ferromagnetic chamber material of 0.75 mm thickness. The peak fields measured were the radial flux density on the outside surface of the discharge chamber at a location directly adjacent to the sidewall magnet cusp. As indicated, the flux density drops to approximately that of the Earth-field within a 20 cm distance from the chamber wall. Data obtained from measurements of the 1.5 mm and 0.75 mm thick steel chamber material indicated comparable flux densities. Additionally, both 0.75 mm and 1.5 mm thick steel chambers displayed evidence of saturation. The use of a high permeability material in the plasma screen construction may be appropriate to reduce the stray magnetic fields in both conventional and non-ferromagnetic ring-cusp thruster designs if necessary.

An additional activity was pursued to reduce discharge chamber mass and size by reducing the chamber volume. This was done by modifying the conventional cylindrical chamber geometry to that of a conic-section in the upstream half of the discharge chamber, thereby reducing the discharge chamber volume and shell mass by approximately 40 percent from the baseline cylindrical geometry. The new chamber geometry maintains the same spatial orientation of the permanent magnets, and the same cusp geometry, as that of the baseline thruster. This modification was motivated by the observation that typically $\rangle$ 90% of the electron current is collected at the magnetic cusps, with very low electron or ion flux measured at the upstream chamber boundaries. Consequently these surfaces tend to contribute to shaping of the discharge magnetic field and to neutral atom confinement, and do not represent a significant loss area for primary electron current or ion recombination. Tests conducted with this geometry chamber indicate no appreciable reduction in discharge performance over that of the baseline cylindrical chamber, as indicated in Fig. 10. Additionally, no substantiative changes in ion optics perveance or beam profile were observed. Consequently, development of a thruster with a 'partial-conic' chamber is anticipated. This geometry has the additional benefit of being considerably stronger that the conventional flat-backplate thruster design.

It is of interest to note that an additional discharge chamber mass reduction can be obtained by simply reducing the thruster chamber length. However, using this approach, a mass reduction-versus-engine performance and lifetime tradeoff is realized. In addition to reducing the thruster mass, reductions in the chamber length increase the neutral loss rate. This in turn reduces the maximum obtainable propellant efficiency and overall thruster efficiency, and increases the charge-exchange ion production rate and consequently accelerator grid erosion rate. The impact of chamber length on neutral loss rate is readily apparent when plotting the neutral loss rates for various 30 cm-class beam diameter thrusters versus their respective chamber lengths[17-21], as shown in Fig. 11. All data were normalized to a standard ion optics electrode geometry and beam diameter[1] to account for differences in ion optics neutral transparency from thruster-to-thruster. As indicated a trend of decreased neutral loss rate with increased chamber length is evident. This correlation is to be expected based on a prior analysis.[22] The use of the baseline chamber length of 220 mm is anticipated, as this permits high propellant and thruster efficiency while operating at highly-throttled conditions at low power.

To further reduce the neutral loss rate and boost performance at low power, an alternative location for main propellant injection into the discharge chamber was examined. The baseline thruster incorporates a main propellant plenum on the upstream surface of the discharge chamber. The plenum consists of a ring-shaped feed tube concentric about the discharge cathode assembly located at approximately the half-radius of the discharge chamber, with the propellant injected downstream into the discharge (termed here as 'forward' injection). An additional main plenum was incorporated at the downstream end of the thruster, with the propellant injected axially upstream into the discharge (termed here as 'reverse' injection).

The impact on discharge chamber performance of using 'reverse' versus 'forward' propellant injection is shown in Fig 12. These data were obtained by repeatedly valving a constant main propellant flow rate from one plenum to another during steady-state thruster operation and noting the change in performance. At a constant total propellant flow rate into the thruster, switching from 'forward' to 'reverse' main propellant feed consistently reduced the discharge voltage by ~0.5-1.0 volt, without changing any other thruster parameter. By reducing the discharge voltage for a fixed beam and discharge current, a reduction in discharge power is realized. Since no reduction in beam current is observed with reduced discharge voltage, the propellant injection appears to change the anode-fall voltage.

Conversely, for a fixed beam current and discharge voltage, 'reverse' propellant injection decreases the neutral loss rate by increasing the effective discharge chamber length. The reduced neutral loss rate increases the propellant efficiency. Consequently the use of a 'reverse' propellant feed injection is anticipated in future thruster designs.

Ion Optics

The laboratory model derated ion thruster has been tested using a two-grid ion accelerating system developed for the J-series mercury ion thruster which was designed for primary propulsion functions. These ion accelerating electrodes are dished to provide a preferential and repeatable direction of deformation under thermal loading.[23] Both dish directions (concave and convex) have been evaluated.[23,24] The convex, or outward, dish was selected beacuse it gave an increased ion extraction capability for a given cold electrode spacing. This behavior occurs because the electrode spacing decreases with increasing discharge chamber power and electrode temperature.

This feature is important for primary propulsion because it allows increased vlaues of the thrust-to-power ratio (more beam current for a given beam voltage). However, as reference 2 has shown, the net mass benefit of using ion propulsion for stationkeeping is insensitive to large variations in specific impulse (hence, thrust-to-power ratio) and power level. Consequently, the selection of electrode dish direction may be dictated by some parameter other than thruster performance such as the near-field energetic beam ion envelope.

When the ion accelerating electrodes are fabricated, the relative position of each pair of electrode holes that form an ion beamlet are adjusted or 'compensated' to steer the beamlet in a more axial direction. If uncompensated, the beamlets diverge beacuse of the dished shape of the electrodes and hole pair relative displacement due to the finite electrode thickness and electrode spacing.[23-25] This divergence can lead to thrust losses greater than 10 percent.[25] With compensation, the divergence losses can be reduced to about 2 percent.

Even though the thrust losses can be reduced via compensation, a low current density (typically 1-2 percent of the maximum) of high energy ions is observed at high angles (about 30 degrees) from the beam axis.[26] It is uncertain whether these ions originate from the entire grid surface or from a preferential region such as the beam edge. In either case, if they are emitted from the electrode holes fairly symmetrically and normal to the grid surface, then a dish direction change (from convex to concave or inward) could significantly reduce the beam diameter near the thruster. The beam envelope might be shifted downstream by nearly as much as twice the electrode radius of curvature. For conventional 30 cm diameter ion optics, this would be approximately 1 meter.

New, compensated electrodes have been fabricated and assembled to J-series mounting systems to evaluate any performance and beam envelope variations. The impact of inward-dish electrodes on discharge chamber performance is expected to be small because the change in discharge chamber volume is only about 12 percent. The impact on ion extraction capability of the electrodes is uncertain. Early dished grid studies, using unmounted electrodes, estimated a change in electrode spacing of about 0.26 mm when the electrodes were subjected to thermal loads.[23,24] The spacing decreased for dished-out electrodes and increased for dished-in electrodes. However, later direct measurements with J-series thrusters and complete electrode assemblies yielded spacing decreases of about 0.07 and 0.12 mm, independent of operating power level, for two different sets of electrodes.[27] Thus, the ion extraction capability, or grid-set perveance, with dished-in geometries may be significantly less than that of dished-out geometries.

While the net mass benefits of using ion propulsion for stationkeeping of communication satellites are insensitive to specific impulse as described earlier, the required thruster operating time decreases with specific impulse This occurs because the thrust for a given thruster input power increases as the beam voltage (or specific impulse) decreases. Reduced thruster operating times are desirable because they lead to shorter and less costly qualification tests.

Using two-grid ion optics and operating at a fixed ratio of net-to-total accelerating voltage and constant thruster input power, the thrust can be increased with grid geometry changes that lead to increased ion optics current extraction capability. In general, geometric parameters which have been found to affect ion extraction capability the most are: accelerator grid hole diameter, electrode separation, and electrode thicknesses.[24,28-31] The thrust-to-power ratios will be maximized by thruster operation at or near the minimum pssible total accelerating voltage. These effects are discussed along with their anticipated impact on thruster performance and lifetime.

Ion extraction capability is determined by the onset of accelerator grid impingement current due to beamlet space-charge buildup. Therefore, it is not surprising that accelerator grid hole diameter and hole pair alignment are important parameters. Experimental results from small-area[28,29] and full-size ion optics[24,30,31] are in basic agreement with theoretical analyses of single apertures.[31] In order to extract a two ampere mercury ion beam from 30 cm diameter ion optics, the minimum total accelerating voltage decreased as the accelerator hole diameters were increased

at a rate of about 350 V/mm.[30]

Discharge chamber performance data from reference 30 are replotted in Fig. 13 to show how the discharge chamber propellant efficiency decreased monotonically with increasing accelerator grid hole area for a 30 cm diameter mercury ion thruster. As the discharge voltage was reduced from 36 to 32 volts, to reduce internal erosion, the sensitivity increased from about 7 percentage points per mm^2 change in hole area to 13 percent per mm^2 change. These sensivities may be somewhat different for throttled ring-cusp thrusters operating at discharge voltages $\leq$ 28 volts. However, while the propellant efficiency degradation does not impact the thrust-to-power ratio, it will increase the neutral propellant efflux, charge-exchange ion production rate, and accelerator grid erosion rate. These detrimental effects were observed in the 4350 hour wear test of a 25 cm diameter xenon ion thruster.[4] Reference 4 also showed that as the accelerator grid hole diameter was increased, the minimum accelerator grid voltage to prevent beam electrons from streaming into the discharge chamber also increased by more than 200 V/mm. Thus, increases in the accelerator hole diameter would lead to higher ion impingment energies and shorter grid lifetimes. In summary, the perveance advantages of increasing the accelerator grid hole diameters must be carefully weighed against the performance and lifetime degradation.

An experimental study of the effects of ion accelerator system geometry in ion extraction capability was conducted using 18 different 30 cm diameter two-grid assemblies.[24] Theoretical analyses as well as experimental results from that effort showed that the minimum total ion accelerating voltage, and thus specific impulse, required to extract a given beam current decreased as the electrode spacing or ion accelerating distance was reduced. The lower total accelerating voltages required by the derated ion thruster should allow electrode spacings to be reduced and, hence realization of increased ion extraction capability. This action would permit operation at thrust-to-power ratios greater than those obtained at the standard electrode spacing of about 0.6 mm. Based on voltage breakdown studies of ion accelerator systems[29,32], the margin between the operating condition and the maximum allowable electric field strength should not change as long as the electrode spacing is not reduced to the point of increasing the electric field strength beyond the initial condition. Reduced electrode spacing should not impact thruster lifetime.

Assuming no difficulties in maintaining electrode spacing uniformity or hole pair alignment, reductions in the screen and accelerator grid thicknesses and hole sizes, in proportion with the electrode spacing reduction, should be feasible. Theoretical analyses and experimental results have demonstrated that the normalized perveance per hole is unchanged when all dimensions are scaled down. As an example, if the active-area electrode dimensions of the present derated thruster are reduced by 20 percent then the area of each hole is reduced and the number of holes per grid set is increased by 56 percent. Thus, the total ion current capability should also increase by 56 percent, or more if smaller than scaled grid spacings are feasible. At a constant beam current this ion extraction capability increase would be expected to allow a reduction in total accelerating voltage to about 70 percent of the unscaled value. If all this voltage reduction is permitted to be transfered to the net accelerating voltage then the specific impulse would decrease by about 15 percent. Because thruster power efficiency would decrease with decreasing net accelerating voltage and constant beam current, the net improvement in the thrust-to-power ratio would always be less than the specific impulse decrease but would be about 10 percent depending on the initial net voltage and the ionization and fixed power losses. Thus, the reduction in thruster operating time would be about 10 percent for a 20 percent reduction in ion accelerating electrode dimensions.

Cathodes

For state-of-the-art hollow cathodes that use porous tungsten inserts impregnated with a low work function material, upper and lower temperature limits exist which ensure adequate lifetime and electron emission stability.[33,34] Temperatures in the range of about 1050 to 1100 degrees centigrade are desired at the cathode tube-orifice plate junction prior to cathode ignition and during normal operation. Cathodes used in the derated thruster require heater power to prepare the cathode and insert for discharge ignition. After discharge ignition, the heater power is removed, the cathode temperature is maintained by ion bombardment from the plasma discharge, and electrons are drawn from the insert to the discharge chamber anode surfaces. Figure 14 presents data obtained from four cathodes with varying orifice geometries and shows how the cathode tube or orifice plate edge temperature varied with emission current. Temperature measurements were obtained using a 2-color pyrometer. The data for the 1.47 mm orifice diameter cathode agrees well with those from reference 33 for a similar cathode size used in 5 kW-class xenon ion thrusters. Temperatures beyond the desired range lead to life-limiting reaction and evaporation rates while those below ~900 degrees centigrade lead to unstable and nonrepeatable operation. This problem can be addressed by correct selection of the cathode orifice diameter, as implied by the data of Fig. 14.

At an emission current of 6 amperes, approximately the derated thruster operating condition at an input power of 640 watts, a cathode orifice diameter of about 0.75 mm

should yield an optimal cathode thermal environment. This cathode orifice diameter is equivalent to that developed for SEPS mercury ion thrusters which accumulated more than 60,000 hours of operation.[35]

Cathode orifice erosion rates for mercury and xenon propellants have been shown to decrease with decreasing ratios of emission current-to-orifice diameter. Immeasurable erosion rates ($< 10^{-5}$ m increase per 1000 hours of testing) of the orifice diameter were experienced in 5 and 10 kW xenon ion thruster tests of 900 and 227 hours, respectively, when the ratios of emission current-to-orifice diameter were 12 and 21 A/mm.[36,37] An average erosion rate of 5.6×10^{-5} m/kHr was obtained when a cathode was operated on xenon for 5000 hours.[38] The final current-to-orifice diameter ratio was 12 A/mm, which is the criterion specified in reference 32 as an upper limit to avoid cathode orifice erosion with mercury propellant. Therefore a xenon cathode operating at about 6 amperes of emission current and having a 0.75 mm diameter orifice should not experience orifice erosion.

To summarize, long-life hollow cathodes appropriate for use in the derated ion thruster over its full power throttling envelope are available. Depending upon the specific thruster application and operating power level, the discharge and neutralizer cathode orifice size is selected and implemented according to the total emission current requirement, consistent with the operating temperature and orifice plate erosion criteria.

Performance Assessment

The overall thruster efficiency versus specific impulse for the derated thruster on xenon propellant is shown in Fig. 15, for beam-to-total voltage (R-ratio) ratios from 0.40-to-0.80. As indicated, the derated thruster efficiency varies from approximately 40 percent at 1500 seconds, to 65 percent at 3000 seconds. The maximum thruster input power and beam power are plotted in Fig. 16, over the same specific impulse range indicated in Fig. 15. These data were obtained at the highest thrust-to-power ratio operating condition for the corresponding specific impulse value. As indicated, the maximum input power varies from approximately 500 watts at 1500 seconds, to in-excess-of 3000 watts at 3000 seconds. As the ion optics electrode spacing was gapped for ~5 kW operation, some modest increase in perveance, and hence input and beam power levels would be anticipated from those indicated in Fig. 16 by reducing the electrode spacing. However increases of 100% or more in power handling capability (at a fixed specific impulse) beyond that indicated in Fig. 16 for 30 cm ion thruster technology are not expected. If developments would allow for significant increases in current and power density, other factors such as lifetime may conspire to push the density down.

The performance impacts of engine throttling include variations in baseline discharge losses, and maximum obtainable discharge and total propellant efficiencies. The variation in discharge losses versus thruster input power is illustrated in Fig. 17. As indicated, the discharge losses decrease with increasing input power. This behavior is explained by the fact that at increasing input power, higher electron and neutral densities are present in the discharge which result in a higher collision frequency and ionization rate. At lower input power levels, there are lower discharge densities, resulting in a higher rate of electron loss to anode potential surfaces without undergoing inelastic collisions. As the discharge power becomes an ever-increasing fraction of the total thruster input power at low values of specific impulse, the electrical efficiency of the thruster decays. Also plotted in Fig. 17 are values of discharge losses for several other stationkeeping and primary propulsion thrusters.[19,21,39-42] As indicated in Fig. 17, the derated ion thruster operates at lower discharge losses, and hence must dissipate less power, than virtually all other xenon ion thrusters over the 300 watt-to-6000 watt power envelope.

When the total propellant flow to the thruster is reduced at a throttled operating condition, the maximum obtainable propellant efficiency for a fixed discharge voltage (fixed electron energy) is reduced. This is because for a fixed thruster geometry a constant neutral loss rate is experienced. This is illustrated in Fig. 18, a plot of nominal discharge chamber propellant efficiency versus input power. The propellant efficiency values plotted in Fig. 18 correspond to the discharge losses plotted in Fig. 17. As indicated, the derated thruster discharge propellant efficiency varies from approximately 80-to-92% over the 300 watt-to-6000 watt power envelope. Also plotted in Fig. 18 are discharge propellant efficiency values for other stationkeeping and primary propulsion ion thrusters[19,21,39-42]. As indicated, the derated ion thruster operates at higher propellant efficiencies than most all other xenon ion thrusters. The exception to this are some operating conditions of the UK-10 thruster, operated at high discharge voltage. From the perspective of overall thruster performance, the derated engine operates at substantially higher thrust levels than conventional stationkeeping thrusters for the same input power.[1]

Lifetime Assessment

First-order estimates of lifetime can be established for the derated ion thruster using simple analyses[1] and comparisons to weartest results.[36] This is done here for the

operational power range of the thruster.

Fundamental life-limiting phenomena of ion thrusters include erosion of discharge chamber cathode potential surfaces (primarily the screen grid) by discharge ions, and erosion of the accelerator grid by charge-exchange ions. In the derated thruster operating at power levels appropriate to auxiliary propulsion, the erosion rates associated with these phenomena are extremely low due to the low current densities and electrode voltages. The magnitude of these erosion mechanisms are however a strong function of the thruster input power as the following analyses illustrates.

Figure 19 shows the projected lifetime of the screen grid, accelerator grid, and discharge hollow cathode for the derated thruster operating at the indicated power ranges. The methodology employed to estimate the relative screen and accelerator grid lifetimes versus power is that outlined in reference 1. To obtain an absolute measure of estimated lifetimes, the calculated erosion rates were normalized to those measured during an extended-duration weartest of a high power xenon ion thruster from reference 36.

The erosion of the screen grid is assumed to be a result of singly- and doubly-charged discharge chamber ion sputtering, with an end-of-life occurring defined to be at a condition where the screen electrode is eroded to half of its original 360 micron thickness. The erosion of the accelerator grid is assumed to be a result of charge-exchange ion sputtering, with an end-of-life occurring at a condition prior to loss of the accelerator electrode structural integrity. This will occur at some point beyond a mass loss of 100 grams, from a 24 percent open-area-fraction, 30 cm diameter, 510 micron-thick molybdenum electrode. This total mass loss value criteria was obtained from the post-test examination of weartest accelerator grid electrodes, including that of reference 37, which have experienced total mass losses exceeding 100 grams from beginning-of-life, without failure. Additionally, a limiting criterion to hollow cathode lifetime was included. This criterion was a maximum total emission current capability of 396 kA-hr, based on the longest total demonstrated operation of a single impregnated insert device of an ion thruster hollow cathode.[43]

The data of Fig. 19 indicate that for derated thruster input power levels less than ~5 kW, the life-limiting component is potentially the hollow cathode, as the known erosion mechanisms for screen and accelerator grid erosion become diminishing small. For input power levels >5 kW, accelerator grid erosion due to charge-exchange ions appears to be the life-limiting phenomenon. Additionally, for input power levels up to 5.5 kW, the projected derated thruster lifetimes (>12,000 hours) are in excess of that required to conduct auxiliary, and near-Earth space primary propulsion functions.

Conclusions

Activities to develop and refine a 30 cm engineering-model derated ion thruster were described. The approach is to develop a thruster capable of performing both auxiliary and primary propulsion functions in the 0.5-5.0 kW power range. Design modifications to the discharge chamber of the 30 cm derated ion thruster indicate significant reductions in thruster mass and volume, without performance degradation, are obtainable. This thruster mass optimization activity was motivated by the an analysis which indicates a strong sensitivity of spacecraft mass in GTO to thruster mass.

Design modifications to two-grid ion accelerating electrodes to reduce mass and improve performance at derated thruster operating conditions without impacting lifetime include scaling the electrode separation, hole sizes, and thicknesses. A 20 percent reduction in all dimensions would be expected to lead to a 15 percent reduction in specific impulse and a 10 percent increase in the thrust-to-power ratio. Therefore, the thruster operating time for a given mission would also decrease by about 10 percent.

As the target thruster power level is changed based on the propulsion application, the cathode emission current requirement is changed, requiring a modification to the cathode orifice diameter to maintain an optimal operating temperature. Prior extended duration tests of mercury and xenon hollow cathodes with orifice diameters and emission currents over the power envelope of the derated thruster have verified the longevity of the hollow cathodes proposed for the thruster.

The maximum input power and beam power were quantified for the derated thruster over a broad range in specific impulse. The maximum input power varies from approximately 500 watts at 1500 seconds to greater than 3000 watts at 3000 seconds, on xenon propellant. The performance impacts of engine throttling were quantified, including the variation in discharge losses and discharge chamber propellant efficiency with input power. The discharge chamber performance of the derated thruster was found to be superior to most other auxiliary and primary propulsion xenon ion thrusters over a 300 watt-to-6000 watt power envelope.

First-order estimates of derated thruster lifetime were made based on analyses of critical component erosion and weartest results. Thruster lifetimes of greater than 12,000 hours are projected for input power levels up to 5.5 kW. These lifetimes are in excess of that required to conduct auxiliary and near-Earth space primary propulsion functions.

References

[1]Patterson, M.J. and Foster, J.E., "Performance and Optimization of a 'Derated' Ion Thruster for Auxiliary Propulsion," AIAA Paper, AIAA Paper No. 91-2350, June 1991.

[2]Rawlin, V.K. and Majcher, G.A., "Mass Comparisons of Electric Propulsion Systems for NSSK of Geosynchronous Spacecraft," AIAA Paper No. 91-2347, June 1991.

[3]Day, M.L., et. al., "INTELSAT VII Ion Propulsion Subsystem Implementation Study," AIAA Paper No. 90-2550, July 1990.

[4]Beattie, J.R., Matossian, J.N., and Robson, R.R., "Status of Xenon Ion Propulsion Technology," AIAA Paper No. 87-1003, May 1987.

[5]Brophy, J.R. and Aston, G., "A Detailed Model of Ion Propulsion Systems," AIAA 89-2268, July 1989.

[6]Beattie, J.R., "Status of Xenon Ion Propulsion Technology for Stationkeeping," presented at the INTELSAT Electric Propulsion Symposium, June 1991.

[7]"Development of the Ion Propulsion System for ETS-VI." presented at the INTELSAT Electric Propulsion Symposium, June 1991.

[8]"The Ion Propulsion Package (IPP) for the ESA Artemis Satellite," presented at the INTELSAT Electric Propulsion Symposium, June 1991.

[9]Fearn, D.G., "The UK-10 Ion Propulsion System Status and Applications," presented at the INTELSAT Symposium on Ion Propulsion for Communication Satellites, July 1989.

[10]Bassner, H., "Status of the RITA Ion Propulsion Assembly," presented at the INTELSAT Electric Propulsion Symposium, June 1991.

[11]Smith, P., "Design and Development of the UK-10 Ion Propulsion Subsystem," IEPC Paper No. 88-033, October 1988.

[12]"30-Centimeter Ion Thruster Subsystem Design Manual," NASA TM 79191, June 1979.

[13]Brophy, J.R., "Ion Thruster Performance Model," NASA CR-174810, December 1984.

[14]Arakawa, Y. and Yamada, T., "Monte Carlo Simulation of Primary Electron Motions in Cusped Discharge Chambers," AIAA Paper No. 90-2654, July 1990.

[15]Feng, Yu-Cai and Wilbur, P.J., "The Influence of Strong Magnetic Fields on Ion Beam Neutralization," AIAA Paper No. 82-1945, November 1982.

[16]Patterson, M.J. and Mohajeri, K., "Neutralizer Optimization," IEPC Paper No. 91-151, October 1991.

[17]Rawlin, V.K., "Internal Erosion Rates of a 10-kW Xenon Ion Thruster," AIAA Paper No. 88-2192, July 1988.

[18]Patterson, M.J. and Rawlin, V.K., "Performance of 10-kW Class Xenon Ion Thrusters," AIAA Paper No. 88-2914, July 1988.

[19]Yamagiwa, Y., et. al., "A 30-cm Diameter Xenon Ion Thruster - Design and Initial Test Results," IEPC Paper No. 88-095, October 1988.

[20]Beattie, J.R. and Matossian, J.N., "High-Power Xenon Ion Thrusters," AIAA Paper No. 90-2540, July 1990.

[21]Martin, A.R., Bond, A., and Lavender, K.E., "A UK Large Diameter Ion Thruster for Primary Propulsion," AIAA Paper No. 87-1031, May 1987.

[22]Kaufman, H.R., "Performance Correlation for Electron-Bombardment Ion Sources," NASA TN D-3041, 1965.

[23]Rawlin, V.K., Banks, B.A., and Byers, D.C., "Dished Accelerator Grids on a 30-cm Ion Thruster," *J. Spacecraft and Rockets*, Vol. 10, No. 1, January 1973, pp. 29-35.

[24]Rawlin, V.K., "Studies of Dished Accelerator Grids for 30-cm Ion Thrusters," AIAA Paper No. 73-1086, October 1973 (NASA TM X-71420).

[25]Danilowicz, R.L., et. al., "Measurement of Beam Divergence of 30-Centimeter Dished Grids," AIAA Paper 73-1051, October 1973.

[26]Lathem, W.C., "Particle and Field Measurements on Two J-Series 30-Centimeter Thrusters," AIAA Paper No. 81-0728, April 1981 (NASA TM 81741).

[27]MacRae, G.S., Zavesky, R.J., and Gooder, S.T., "Structural and Thermal Response of 30 cm Diameter Ion Thruster Optics," AIAA Paper No. 89-2719, July 1989.

[28]Aston, G. and Kaufman, H.R., "The Ion-Optics of a Two-Grid Electron Bombardment Thruster," AIAA Paper No. 76-1029, November 1976.

[29]Rovang, D.C. and Wilbur, P.J., "Ion Extraction Capabilities of Two-Grid Accelerator Systems," NASA CR-174-621, 1984.

[30]Rawlin, V.K., "Sensitivity of 30-cm Mercury Bombardment Ion Thruster Characteristics to Accelerator Grid Design," AIAA Paper No. 78-668, April 1978.

[31]Poeschel, R.L., "High Power and 2.5 kW Advanced Technology Ion Thruster," Hughes Research Laboratories, Malibu, California, NASA CR-135163, February 1977.

[32]Kaufman, H.R., "Technology of Electron-Bombardment Ion Thrusters," in *Advances in Electronics and Electron Physics*, Vol. 36, Academic Press, Inc., New York, 1974, pp. 308-310.

[33]Verhey, T.R. and Patterson, M.J., "Microanalyses of Extended-Test Xenon Hollow Cathodes," AIAA Paper No. 91-2123, June 1991.

[34]Mirtich, M.J. and Kerslake, W.R., "Long Lifetime Hollow Cathodes for 30-cm Mercury Ion Thrusters," AIAA Paper No. 76-985, November 1976.

[35]Rawlin, V.K., "Advanced Ion Propulsion for Space Exploration," AIAA Paper No. 91-3567, September 1991.

[36]Patterson, M.J. and Verhey, T.R., "5 kW Xenon Ion Thruster Lifetest," AIAA Paper No. 90-2543, July 1990.

[37]Rawlin, V.K., "Internal Erosion Rates of a 10 kW

Xenon Ion Thruster," AIAA Paper No. 88-2912, July 1988.

[38]Brophy, J.R. and Garner, C.E., "A 5000 Hour Xenon Hollow Cathode Life Test," AIAA Paper No. 91-2122, June 1991.

[39]Shimada, S., et. al., "Ion Engine System Development of ETS-VI," AIAA Paper No. 89-2267, July 1989.

[40]Kitamura, S., Miyazaki, K., and Hayakawa, Y., "1000 Hour Test of 14 cm Diameter Ring-Cusp Xenon Ion Thruster," AIAA Paper No. 90-2542, July 1990.

[41]Smith, P., "Design and Development of the UK-10 Ion Propulsion Subsystem," AIAA Paper No. 88-033, Ocotber 1988.

[42]Fearn, D.G., Martin, A.R., and Smith, P., "Ion Propulsion Research and Development in the UK," IAF Paper No. 89-274, Ocotber 1989.

[43]Personal communication, Mantenieks, M., NASA Lewis Research Center, August 1991.

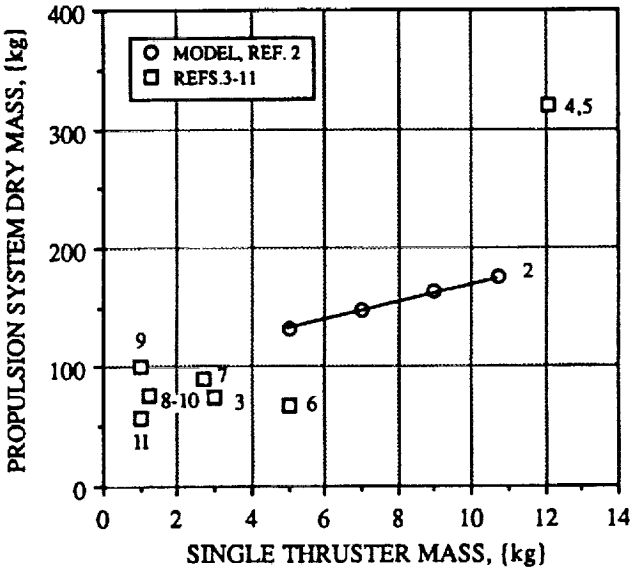

Fig. 1 Propulsion system dry mass vs. single thruster mass.

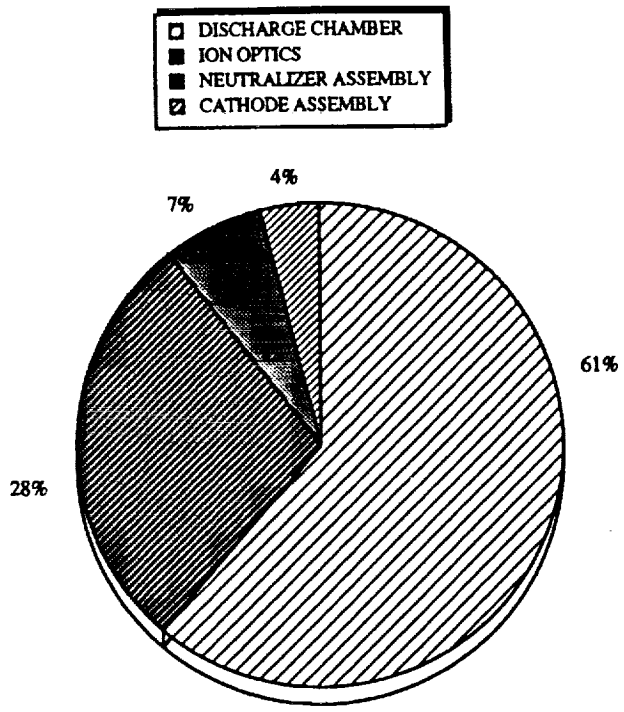

Fig. 3 Mass-breakdown of 30 cm laboratory model derated ion thruster.

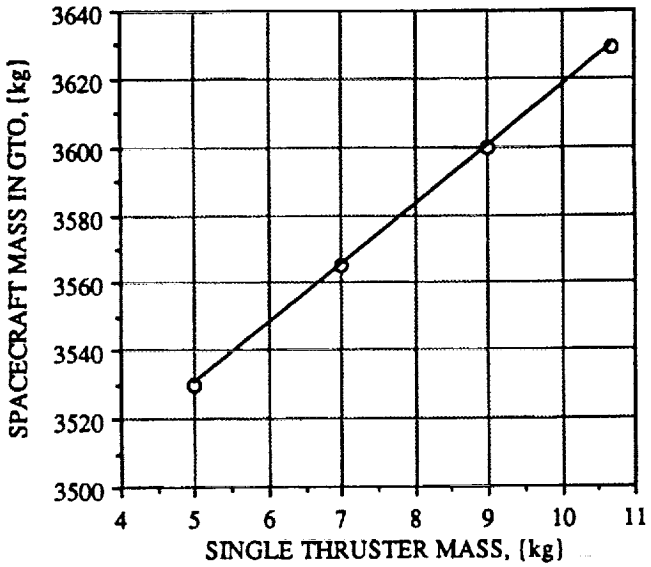

Fig. 2 Spacecraft mass in GTO vs. single thruster mass.

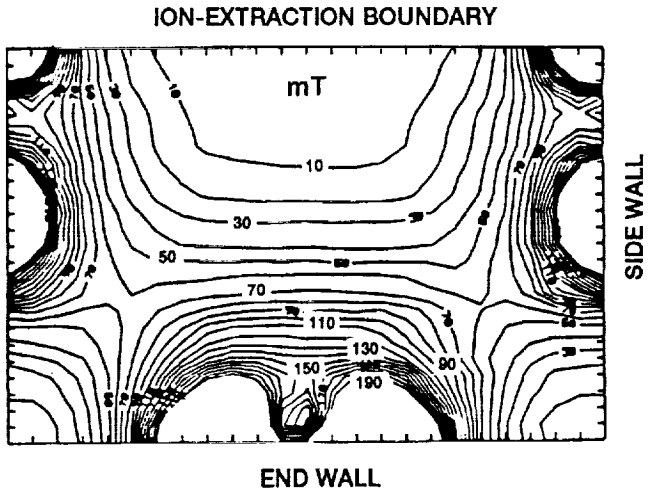

Fig. 4 Scalar magnetic field contour plot of ring-cusp discharge chamber; 1.5 mm thick chamber wall.

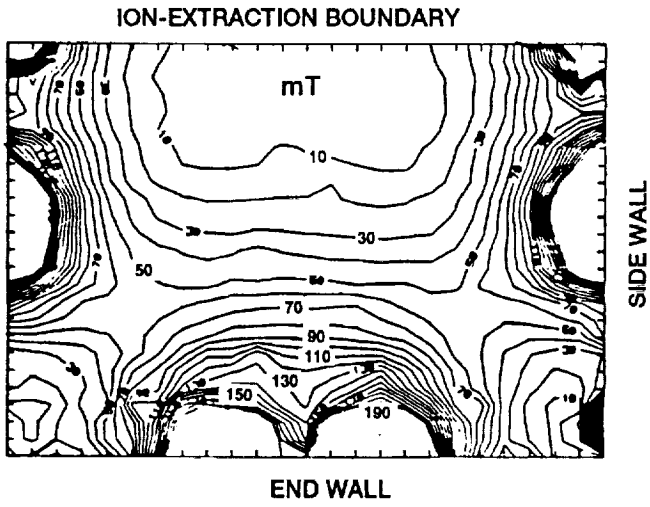

Fig. 5 Scalar magnetic field contour plot of ring-cusp discharge chamber; 0.75 mm thick chamber wall.

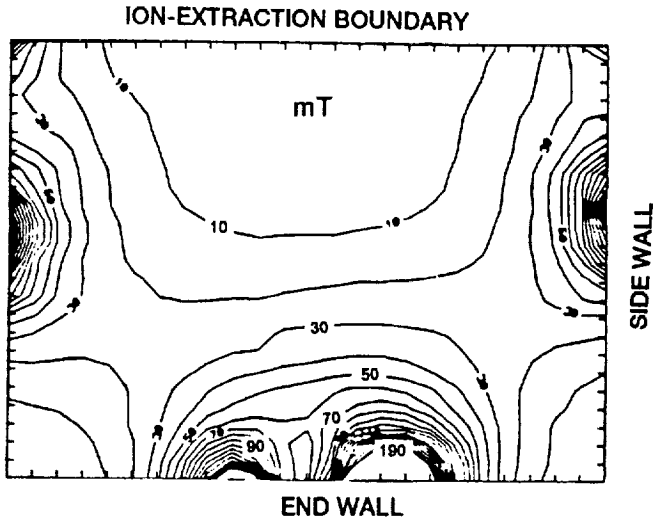

Fig. 7 Scalar magnetic filed contour plot of ring-cusp discharge chamber; 0.75 mm thick chamber wall, with reduced-size permanent magnets.

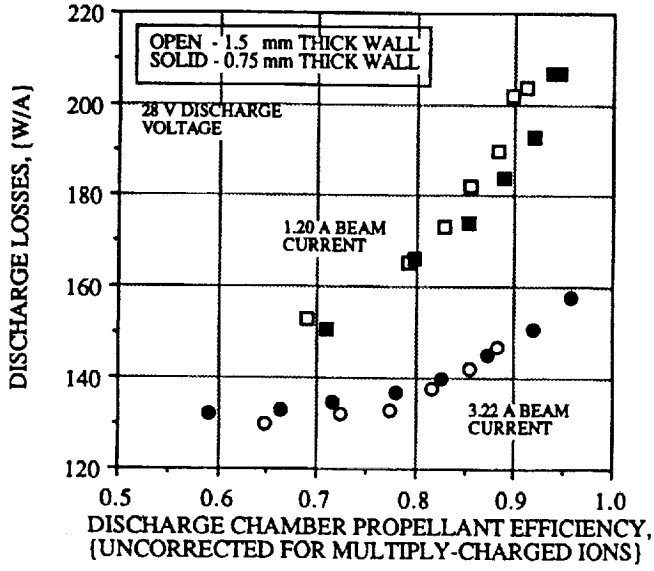

Fig. 6 Discharge chamber performance for 1.5 mm and 0.75 mm thick chamber wall thicknesses.

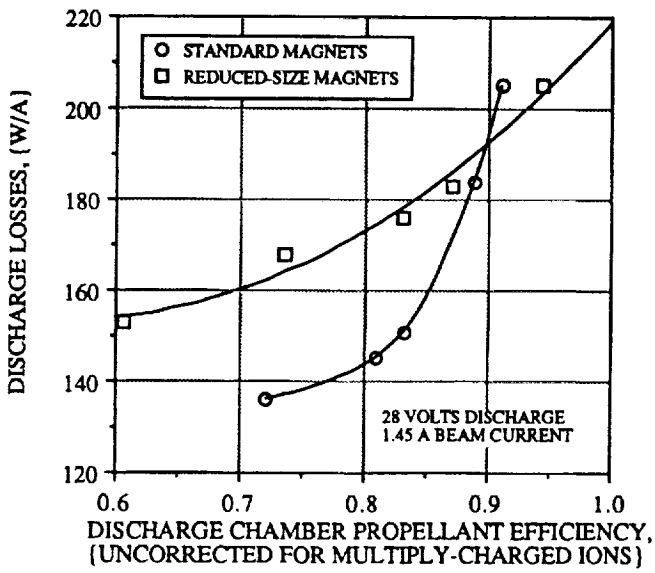

Fig. 8 Discharge chamber performance for standard and reduced-size permanent magnets.

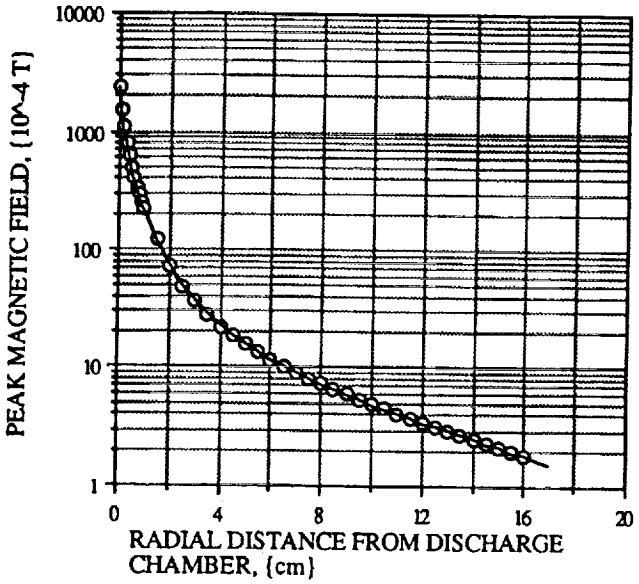

Fig. 9 Peak thruster external magnetic field vs. distance.

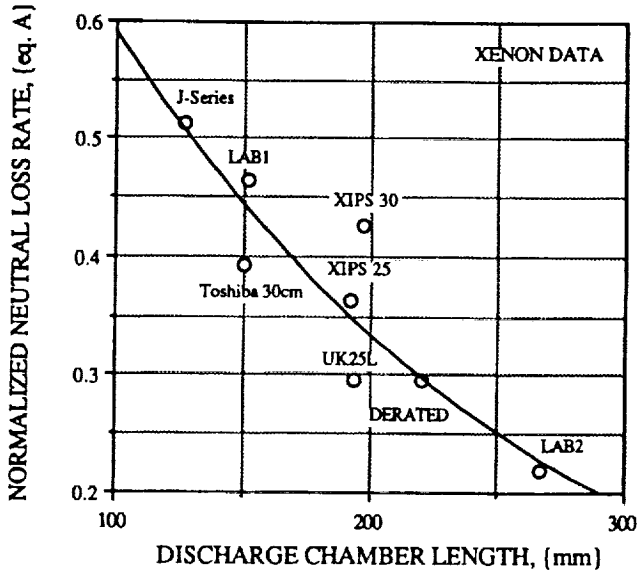

Fig. 11 Neutral loss rate vs. discharge chamber length; xenon data.

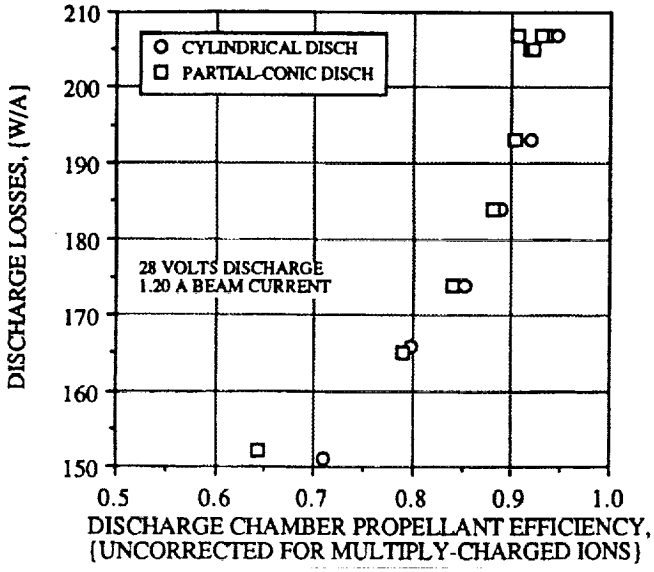

Fig. 10 Discharge chamber performance for cylindrical and conic discharge chamber geometries.

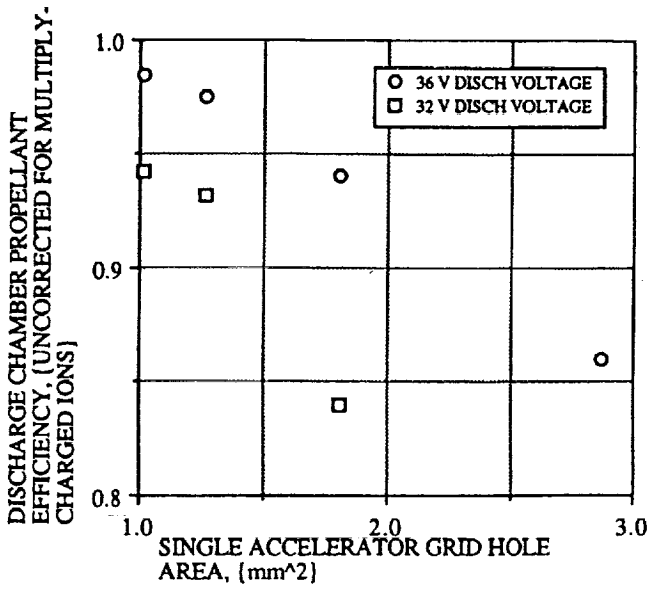

Fig. 12 Discharge chamber propellant efficiency vs. accelerator grid hole area.

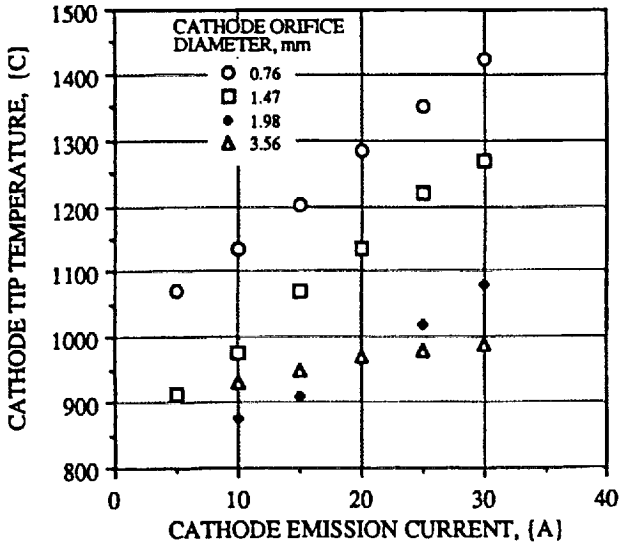

Fig. 13 Hollow cathode tip temperature vs. emission current.

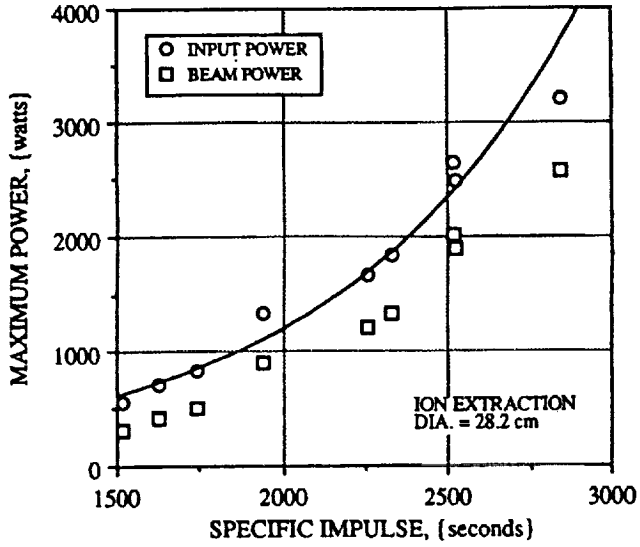

Fig. 15 Maximum imput power and beam power vs. specific impulse.

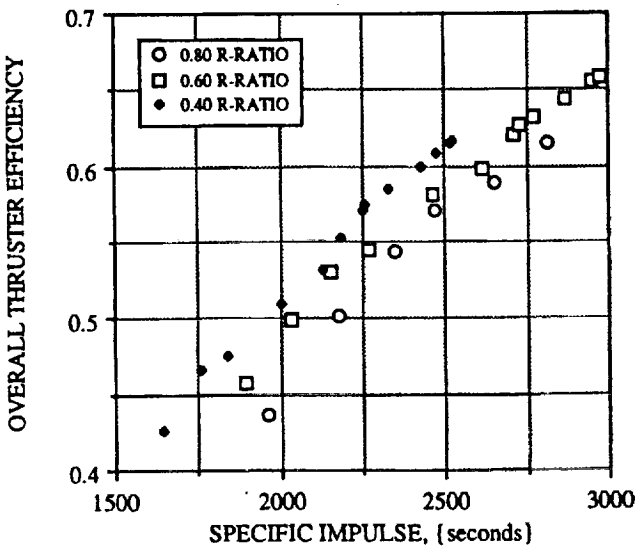

Fig. 14 Thruster efficiency vs. specific impulse.

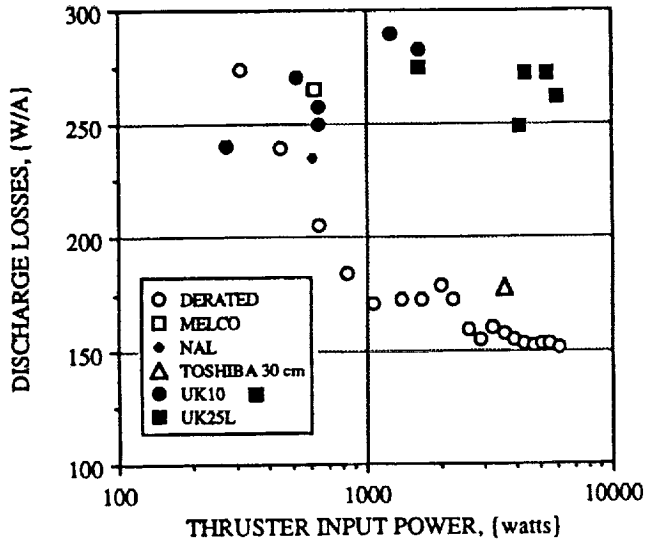

Fig. 16 Variation in discharge losses vs. thruster input power.

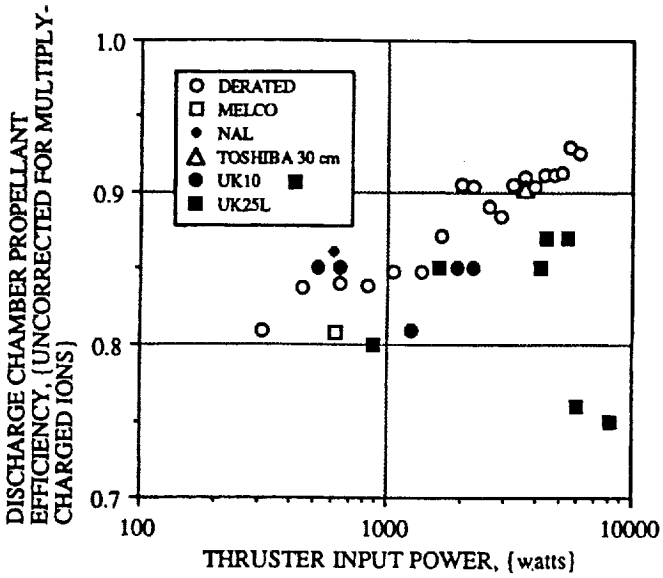

Fig. 17 Discharge chamber propellant efficiency vs. thruster input power.

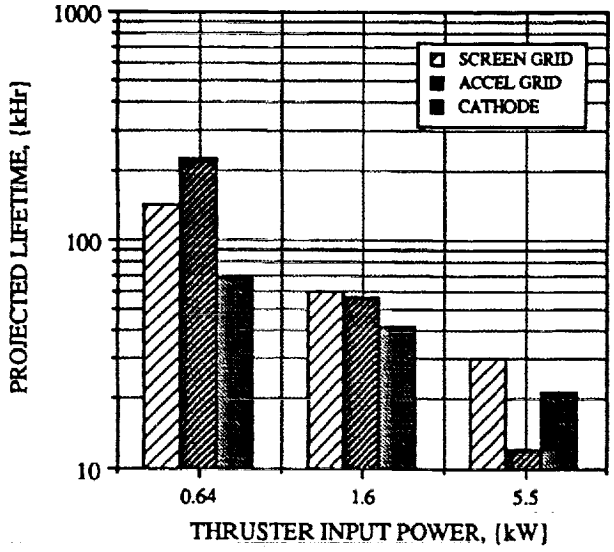

Fig. 18 Projected thruster component lifetime vs. input power.

REPORT DOCUMENTATION PAGE

Form Approved
OMB No. 0704-0188

1. AGENCY USE ONLY (Leave blank)	2. REPORT DATE	3. REPORT TYPE AND DATES COVERED
	October 1991	Technical Memorandum

4. TITLE AND SUBTITLE
Derated Ion Thruster Design Issues

5. FUNDING NUMBERS
WU-506-42-31

6. AUTHOR(S)
Michael J. Patterson and Vincent K. Rawlin

7. PERFORMING ORGANIZATION NAME(S) AND ADDRESS(ES)
National Aeronautics and Space Administration
Lewis Research Center
Cleveland, Ohio 44135-3191

8. PERFORMING ORGANIZATION REPORT NUMBER
E-6902

9. SPONSORING/MONITORING AGENCY NAMES(S) AND ADDRESS(ES)
National Aeronautics and Space Administration
Washington, D.C. 20546-0001

10. SPONSORING/MONITORING AGENCY REPORT NUMBER
NASA TM-105576

11. SUPPLEMENTARY NOTES
Prepared for the 22nd International Electric Propulsion Conference, co-sponsored by the AIDAA, AIAA, DGLR, and JSASS, Viareggio, Italy, October 14-17, 1991. Responsible person Michael J. Patterson, (216) 433-7481.

12a. DISTRIBUTION/AVAILABILITY STATEMENT
Unclassified - Unlimited
Subject Category 20

12b. DISTRIBUTION CODE

13. ABSTRACT *(Maximum 200 words)*

Preliminary activities to develop and refine a lightweight 30 cm engineering-model ion thruster are discussed. The approach is to develop a "derated" ion thruster which is a thruster capable of performing both auxiliary and primary propulsion roles over an input power range of at least 0.5-5.0 kW. Design modifications to a baseline thruster to reduce mass and volume are discussed. Performance data over an order-of-magnitude input power range are presented, with emphasis on the performance impact of engine throttling. Thruster design modifications to optimize performance over specific power envelopes are discussed. Additionally, lifetime estimates based on weartest measurements are made for the operating envelope of the engine.

14. SUBJECT TERMS
Ion thruster; Xenon ion propulsion; Auxiliary propulsion

15. NUMBER OF PAGES
16

16. PRICE CODE
A03

17. SECURITY CLASSIFICATION OF REPORT	18. SECURITY CLASSIFICATION OF THIS PAGE	19. SECURITY CLASSIFICATION OF ABSTRACT	20. LIMITATION OF ABSTRACT
Unclassified	Unclassified	Unclassified	